

Old Dominion University

ODU Digital Commons

Physics Faculty Publications

Physics

7-2020

Multi-Metallic Conduction Cooled Superconducting Radio-Frequency Cavity with High Thermal Stability

Gianluigi Ciovati

Gary Cheng

Uttar Pudasaini

Robert A. Rimmer

Follow this and additional works at: https://digitalcommons.odu.edu/physics_fac_pubs



Part of the [Condensed Matter Physics Commons](#)

Letter

Multi-metallic conduction cooled superconducting radio-frequency cavity with high thermal stability

Gianluigi Ciovati^{1,2} , Gary Cheng¹, Uttar Pudasaini³ and Robert A Rimmer¹¹ Thomas Jefferson National Accelerator Facility Newport News VA 23606 United States of America² Center for Accelerator Science Department of Physics Old Dominion University Norfolk Virginia 23529 United States of America³ The College of William & Mary Williamsburg VA 23185 United States of AmericaE-mail: gciovati@jlab.org

Received 29 January 2020, revised 25 March 2020

Accepted for publication 27 April 2020

Published 15 May 2020



Abstract

Superconducting radio-frequency cavities are commonly used in modern particle accelerators for applied and fundamental research. Such cavities are typically made of high-purity, bulk Nb and with cooling by a liquid helium bath at a temperature of ~ 2 K. The size, cost and complexity of operating a particle accelerator with a liquid helium refrigerator make the current cavity technology not favorable for use in industrial-type accelerators. We have developed a multi-metallic 1.495 GHz elliptical cavity conductively cooled by a cryocooler. The cavity has a ~ 2 μm thick layer of Nb₃Sn on the inner surface, exposed to the rf field, deposited on a ~ 3 mm thick bulk Nb shell and a bulk Cu shell, of thickness ≥ 5 mm deposited on the outer surface by electroplating. A bolt-on Cu plate 1.27 cm thick was used to thermally connect the cavity equator to the second stage of a Gifford-McMahon cryocooler with a nominal capacity of 2 W at 4.2 K. The cavity was tested initially in liquid helium at 4.3 K and reached a peak surface magnetic field of ~ 36 mT with a quality factor of 2×10^9 . The cavity cooled by the cryocooler achieved a peak surface magnetic field of ~ 29 mT, equivalent to an accelerating gradient of 6.5 MV m^{-1} . The conduction-cooled cavity could be operated in continuous-wave with as high as 5 W dissipation in the cavity for 1 h without any thermal breakdown, because of the Cu outer layer with high thermal conductivity. This result represents a paradigm shift in the technology of superconducting accelerator cavities.

Keywords: radio-frequency cavities, cryocooler, conduction cooling

(Some figures may appear in colour only in the online journal)

1. Introduction

Superconducting radio-frequency (SRF) cavities made of high-purity (residual resistivity ratio, *RRR*, >250) bulk Nb

are one of the building blocks of modern particle accelerator facilities for applied and fundamental research throughout the world [1]. Such cavities have different geometries, depending on the speed and type of particle they are designed to accelerate, the operating frequency is in the gigahertz range and they are surrounded by vessels containing liquid He (LHe) which cools and maintains the cavity surface at ~ 2 K during operation in a so-called cryomodule [2, 3]. The size, cost and complexity of a sub-cooled liquid He cryoplant has limited a



Original Content from this work may be used under the terms of the [Creative Commons Attribution 4.0 licence](https://creativecommons.org/licenses/by/4.0/). Any further distribution of this work must maintain attribution to the author(s) and the title of the work, journal citation and DOI.

more widespread application of the SRF technology so far. To the authors' knowledge, out of the estimated $\sim 30\,000$ dedicated industrial particle accelerators worldwide, the only one using the SRF technology is a 9 MeV electron linac for medical isotope production, which uses a commercial liquid He refrigerator with a capacity of 100 W at 4.3 K [4].

The first application of cryocoolers for SRF cryomodules was done in two cryomodules for the Japan Atomic Energy Research Institute Free Electron Laser in 1993, in which they used Gifford-McMahon (GM) cryocoolers to cool two heat shields to 80 K and 40 K, respectively, and to cool down and recondense the boiled-off liquid in the helium tank surrounding a 499.8 MHz cavity [5, 6]. Cryocoolers are reliable, compact, closed-cycle refrigerators which are easier to operate than LHe ones. An example of a cryocooler application is cooling of superconducting magnets in magnetic resonance imaging machines at hospitals. The power capacity of cryocoolers has been increasing in the last few years and models with a capacity of 2 W at 4.2 K are now available. The capital cost per watt of cooling power has also been decreasing such that the capital cost of a 4 K cryocooler-based cooling system is lower than that of a LHe-based system if the total cooling power required is less than ~ 10 W [7].

Recent progress in the development of thin-film Nb_3Sn has resulted in $\beta = 1$ SRF elliptical cavities of frequency greater than 500 MHz achieving moderate accelerating gradients ($E_{acc} \sim 10\text{--}15$ MV m^{-1}) but a much higher quality factor ($Q_0 \sim 10^{10}$) than could be obtained if those cavities were made of just bulk Nb and cooled in LHe at 4.3 K [8]. Such improvements in both cryocoolers and Nb_3Sn SRF cavities may enable the design of compact, low-energy (1–25 MeV) electron accelerators for industrial and medical applications or for compact light sources [9, 10]. An example of such industrial applications is the environmental remediation of flue gases and/or wastewater. A 1 MeV, 1 MW SRF electron accelerator was recently designed for this application, with a cryomodule having a single-cell cavity cooled by conduction using four cryocoolers with a capacity of 1.5 W at 4.3 K [11]. Recent work on the development of SRF cavities conduction cooled by a cryocooler has resulted in a 650 MHz single-cell elliptical cavity made of bulk Nb operating up to an accelerating gradient of 1.5 MV m^{-1} [12], corresponding to a peak surface magnetic field, B_p , of 5.5 mT [13].

Here we describe the preparation and test results of a single-cell elliptical cavity conduction cooled by a two-stage commercial GM cryocooler. Our approach was to deposit a thick, high-purity Cu layer on the outer cavity surface and to minimize the number of joints between the cavity and the 4 K stage of the cryocooler, to maximize the thermal stability of the cavity against quenching of the superconducting state.

2. Development of cavity coatings

The single-cell cavity used for this study was made of large-grain Nb ($RRR \sim 280$) from CBMM, Brazil [14]. The cell shape is that of the end-cell of a High-Gradient cavity (geometry factor $G = 269 \Omega$, shunt impedance $R/Q = 100.3 \Omega$,

ratio of peak surface electric field over the accelerating field $E_p/E_{acc} = 1.77$, ratio of peak surface magnetic field over the accelerating field $B_p/E_{acc} = 4.47$ mT (MV $\text{m}^{-1})^{-1}$, proposed for the 12 GeV Upgrade of the CEBAF accelerator at Jefferson Lab [15]. The design resonant frequency of the TM_{010} accelerating mode is 1.495 GHz. The cavity wall thickness is ~ 2.9 mm and the end flanges are made of pure Nb. The cavity fabrication used standard techniques of the SRF technology such as deep-drawing, milling and electron-beam welding of cavity parts.

2.1. Nb_3Sn inner coating

The coating of the inner surface of the cavity with Nb_3Sn was done together with another single-cell cavity, stacked vertically inside a high-temperature vacuum furnace. The cavity used for this study was at the bottom position. A crucible with 6 g of Sn (99.999% purity from Sigma Aldrich) and 3 g of SnCl_2 (99.99% purity from Sigma Aldrich), packaged inside two pieces of Nb foils, was placed at the bottom flange of the bottom cavity. The top flange of the top cavity was closed with a Nb cover. The setup was assembled inside an ISO 4 clean room and then installed onto the furnace insert [16, 17]. Once the pressure reached 2.7×10^{-3} Pa, the furnace was heated by ramping up the temperature at a rate of 6 $^\circ\text{C min}^{-1}$ until it reached ~ 500 $^\circ\text{C}$. This temperature was then kept constant for one hour and subsequently ramped up at a rate of 12 $^\circ\text{C min}^{-1}$ up to the coating temperature of ~ 1200 $^\circ\text{C}$. The temperature was monitored with sheathed type C thermocouples attached to the cavities at different locations. After maintaining the coating temperature for 3 h, heating ceased, and the furnace was allowed to cooldown gradually. When the furnace temperature reached below 45 $^\circ\text{C}$, the insert was back-filled to 101.3 kPa with nitrogen, and the coated cavities were removed from the deposition system.

2.2. Cu outer coating

Oxygen-free high-conductivity (OFHC) copper is one of the metals which has a higher thermal conductivity than high-purity Nb below 10 K and it has been used as a substrate for the deposition of Nb thin-films on the inner surface of cavities for particle accelerators [18]. The higher thermal conductivity allows for a better thermal stabilization of the cavity, even when cooling with LHe, particularly against the presence of defects in the superconducting thin-film. However, at present there is no technique which allows depositing a thin film of Nb_3Sn directly onto copper with similar performance as achieved by forming the Nb_3Sn layer onto bulk Nb by vapor diffusion.

Nb/Cu bi-metallic samples were produced by electroplating Cu directly onto a Nb and thermal conductivity measurements showed that values of ~ 1 kW (m \cdot K) $^{-1}$ could be achieved at 4.3 K, compared to ~ 75 W (m \cdot K) $^{-1}$ obtained on Nb only [19]. However, achieving such high thermal conductivity depends on obtaining a good adhesion of the Cu on the Nb, which we were not able to achieve reliably and consistently by electroplating Cu directly onto the Nb. A recent

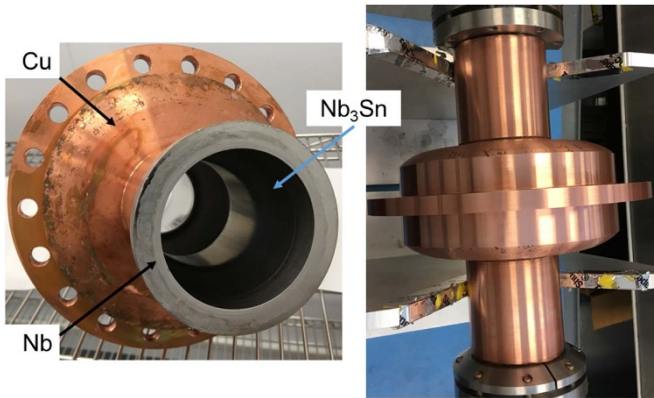


Figure 1. Pictures of the multi-metallic SRF cavity. The length of the cavity from flange to flange is 31.8 cm and the electroplated Cu ring at the equator is 25.4 cm in diameter and 1.27 cm thick.

collaboration between Jefferson Lab, Euclid Techlabs and Concurrent Technologies Corporation (CTC) produced Nb/Cu samples obtained by cold-spraying Cu onto Nb with excellent bonding: a pressure of ~ 40 MPa was required to detach the Cu from the Nb in a pull-adhesion test [20]. However, the thermal conductivity of the cold-sprayed copper was not as high as that obtained by electroplating. While R&D efforts are ongoing towards increasing the thermal conductivity of cold-sprayed copper, we pursued cold-spraying as a method to grow a thin seed layer onto the Nb and then electroplate the copper to full thickness on such layer.

A copper layer ~ 76 μm thick was deposited on the cavity outer surface by cold-spray at CTC, in Johnstown, PA. Copper powder of 99.9% purity and ~ 40 μm size was used along with He as gas carrier. Oxygen-free copper was then electroplated onto the cold-sprayed layer at AJ Tuck Co., in Brookfield, CT. The electroplating was done in several steps to assure that the thickness of the deposited layer was at least 5 mm along the entire cavity contour and finally to grow a ring ~ 25 cm in diameter and ~ 1.3 cm thick at the cavity equator. The cavity was finally machined at Jefferson Lab to remove excess Cu and to make eighteen holes evenly spaced along the Cu ring at the cavity equator. Gore-Tex gaskets were used to seal the cavity ends during both cold-spraying and electroplating, however it was found that some of the copper sulfate plating solution had leaked inside the cavity. The cavity was filled with nitric acid at room temperature for 1 h to dissolve any possible CuSO_4 residue. Figure 1 shows a picture of the completed multi-metallic cavity.

3. Assembly of cavity-cryocooler test stand

A vertical test stand was designed and built to allow testing the cavity with a cryocooler. The GM cryocooler (RDE-418D4, Sumitomo) is bolted to the test stand top plate. The cavity is kept under a static vacuum and sits on a G10 plate held by two stainless steel threaded rods attached to the top plate. A plate ~ 1.27 cm thick machined from OFHC copper is bolted to the cryocooler 4 K stage on one side and to

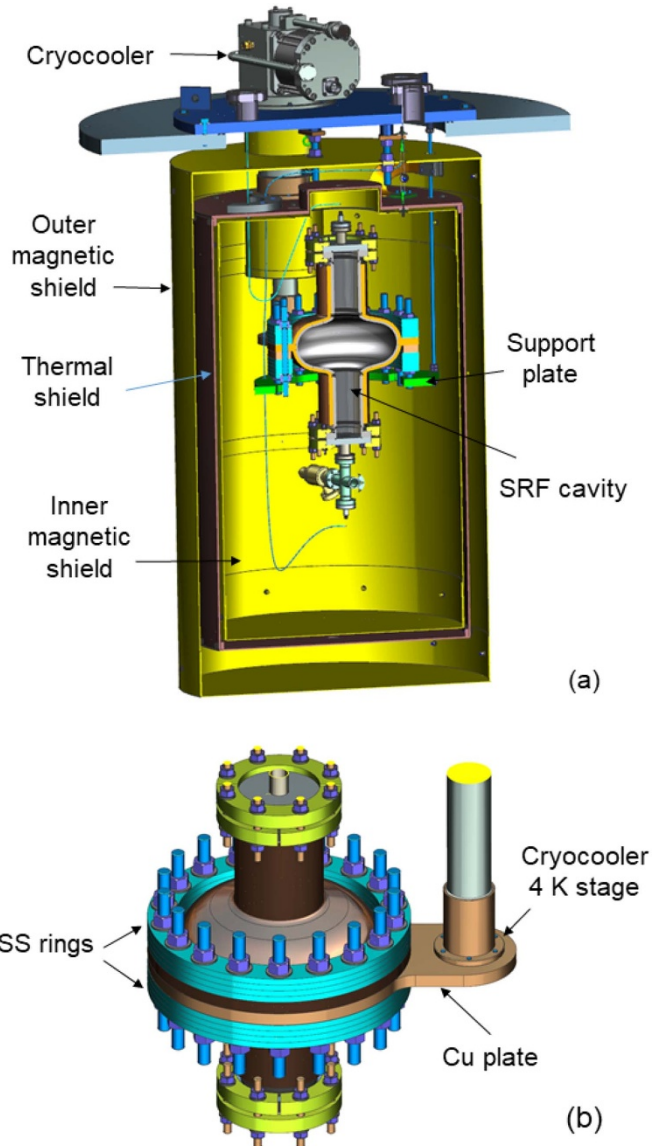


Figure 2. Cross-section of the 3D model of the cavity-cryocooler test stand (a) and detail of the cavity connection to the cryocooler 4 K stage (b). The test stand has a 61 cm diameter top plate and it is 93 cm in height.

the cavity equator ring on the other side. The contact surfaces were cleaned with Brasso metal polish and wiped with acetone and isopropanol. Apiezon N thermal grease was spread on the contact surfaces. The bolts connecting the Cu plate to the cryocooler were torqued to 3 N·m, as recommended by the cryocooler manufacturer. The cavity Cu ring and the Cu plate were sandwiched between four 304 stainless steel rings, each 0.64 cm thick, on each side and pressed together with 1.27 cm diameter, 316 stainless steel threaded rods and silicon-bronze nuts, torqued to 115 N·m. Such a combination of number of rings and torque value allowed achieving a uniform pressure along the ring, estimated to be ~ 46 MPa. A high, uniform pressure allows minimizing the thermal resistance of the joint. Figure 2 shows a 3D rendering of the test stand and of the cavity connected to the cryocooler. Prior to installation onto the cavity, all of the stainless steel hardware had been degaussed

to a remanent magnetic field of less than 20 mG on-contact using a plate type demagnetizer.

The cavity and cryocooler 4 K stage were wrapped with ten layers of multi-layer insulation (MLI) and they are inside an inner magnetic shield. Such inner shield is inside a copper cylinder thermal shield attached to the cryocooler 50 K stage and wrapped with ten layers of MLI. Finally, an outer magnetic shield surrounds the thermal shield. Two rf cables connect the input and pick-up antennae mounted on the cavity to rf feedthroughs on the top plate. Sixteen calibrated Cernox RTDs were distributed on the cavity, Cu plate and the thermal shield. Three cryogenic flux-gate magnetometer probes were placed at locations on the cavity ring with different orientations.

4. Cavity test results

The rf performance was first measured after the deposition of the Nb₃Sn film on the inner surface of the bulk Nb cavity. In preparation for the rf test, the cavity was degreased in an ultrasonic tank, high-pressure rinsed with ultrapure water, assembled with stainless steel flanges with pump-out port and rf feedthroughs and sealed to the cavity with In wire. The cavity was evacuated on a standard vertical test stand to a pressure of $\sim 1 \times 10^{-6}$ Pa before inserting in a vertical cryostat in the Vertical Test Area (VTA) at Jefferson Lab. Cryogenic flux-gate magnetometer (FGM) probes (Mag F, Bartington Instruments) and calibrated Cernox (CX-1010-SD, Lakeshore Cryotronics) resistance-temperature devices (RTDs) were attached to the cavity to monitor the temperature gradient along the cavity and the local magnetic flux density during cooldown close to the critical temperature of Nb₃Sn, $T_c \sim 18$ K. The rf performance of the Nb₃Sn cavity in liquid He at 4.3 K, shown in figure 3, was limited by anomalous heating at 4.3 K starting at $B_p \sim 36$ mT and by thermal quench at $B_p \sim 54$ mT at 2.0 K.

The cavity rf performance was measured again after deposition and machining of the Cu outer layer. The final surface preparation and assembly followed the same steps as after the Nb₃Sn coating, except that an isolation valve was connected between the pump-out port and the pumping line of the vertical test stand. The cavity rf performance was measured in liquid He and it was limited by ‘‘Q-switches’’ at $B_p \sim 35$ mT at 4.3 K, whereas it quenched at $B_p \sim 52$ mT at 2.0 K (figure 3). However, the quality factor degraded more rapidly with increasing field above ~ 14 mT, compared to the test prior to Cu-coating.

After the rf test, the cavity was sealed by closing the valve between the pump-out port and the test stand pumping line. The cavity was then removed from the standard test stand and attached to the one with the cryocooler, as described in section 3. The cavity-cryocooler test stand was inserted in a VTA vertical cryostat, which was used only as a vacuum vessel for this test. The magnitude of the ambient magnetic flux density at the cavity was less than 3 mG. The cooldown lasted about three days and the average steady state temperature of sensors along the Cu plate attached to the cavity equator ring and on top and bottom of the cavity was (3.8 ± 0.4) K. In order to achieve a good thermalization of the cavity in the vicinity of 18 K, which is required in order to minimize rf losses due

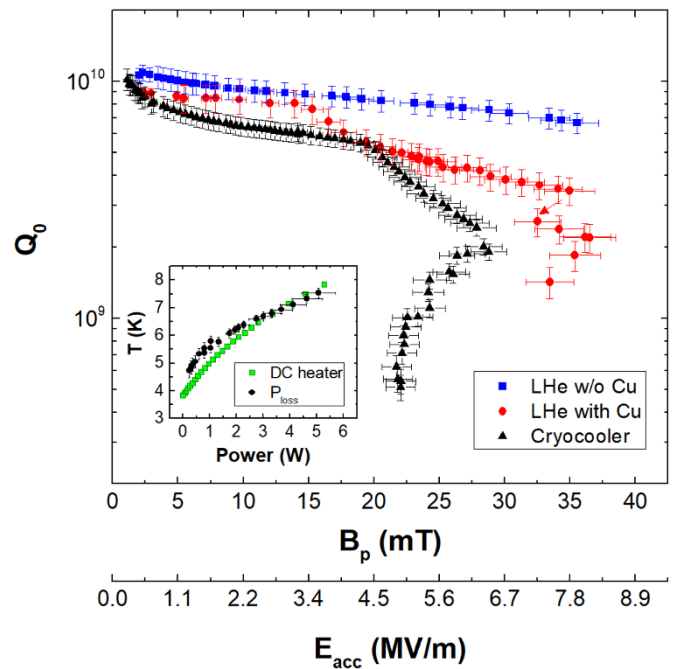


Figure 3. Quality factor of the SRF cavity as a function of the peak surface magnetic field or of the accelerating gradient, in cw mode. The temperature of the outer cavity surface was constant at 4.3 K for the tests in LHe, whereas it increased with increasing rf field in the test with cryocooler. The inset shows the average cavity temperature as a function of the dissipated power, compared with the temperature of a Cu block with a heater mounted to the 4 K stage of the cryocooler as a function of the heater power.

to trapped magnetic flux generated by thermoelectric currents [21], the cryocooler was cycled on and off twice close to this temperature. The maximum magnetic flux density measured by the FGM probes close to T_c was ~ 14 mG and the temperature gradient along the cavity was ~ 0.09 K cm⁻¹.

The Q_0 -value at $B_p = 2.4$ mT was 1×10^{10} and the $Q_0(B_p)$ curve is shown in figure 3 along with the data measured in LHe at 4.3 K before and after Cu coating. The cavity reached a maximum B_p -value of 29 mT above which a Q-switch occurred, reducing both B_p and Q_0 to 22 mT and 5×10^8 , respectively. It was verified that the Q_0 vs. B_p curve is reversible when lowering the forward power. The test was stopped at $P_{loss} = 5$ W, limited by the power handling capability of the input power cable. The cavity was held at this level of dissipated power, corresponding to $Q_0 = 5 \times 10^8$ at 22 mT, for 1 h after which the rf power was turned off. The average cavity temperature, T_{avg} , showed a modest increase from 6.9 K to 7.1 K, as shown in figure 4. There was no indication of thermal instability, such as sudden temperature jumps or dT/dt increasing over time during this extended cavity operation test. All rf tests were done in continuous-wave (cw) mode (100% duty factor) and there were no detectable X-rays from possible field-emitted electrons in any of the tests. The amplitude of the cavity microphonics was measured at $B_p = 10$ mT using the digital low-level rf control system used for the cavity rf test [22] and the peak-to-peak value was 13.8 Hz. The frequency of the microphonics was 1.2 Hz, which is the frequency of the displacer in the 4 K stage of the cryocooler.

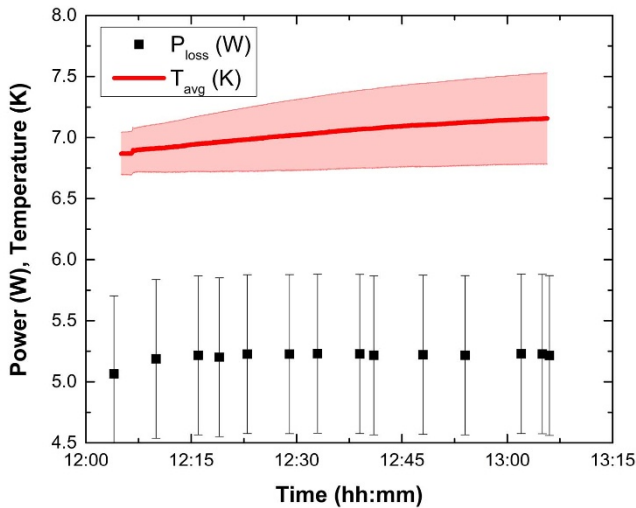


Figure 4. Average temperature of the cavity outer surface while operating the conduction cooled cavity in cw mode with a constant dissipated power of 5 W for 1 h with no indication of thermal instability. The width of the shaded area corresponds to the standard deviation.

5. Discussion

A thermal breakdown of the superconducting state is a common limitation in the operation of SRF cavities in particle accelerators, even when cooled in superfluid He. Except for few exceptions, such thermal breakdown occurs well below the superheating field of the superconductor and it is caused by the presence of defects on the inner cavity surface [23]. An example of such defects are normal conducting inclusions which are heated by the rf field and when the local temperature exceeds T_c the surrounding superconductor quenches. Such quenches can occur even at a relatively low power density. An estimate of the minimum Cu-layer thickness required to reach the highest B_p -value achieved by the cavity tested in LHe after Nb₃Sn coating was carried out using the finite-element computer software ANSYS [24]. The analysis included the heat capacity map of the cryocooler, the temperature- and field-dependent surface resistance (assumed to be uniform) from the cavity test, a contact thermal conductance of 0.7 W/K [25], and estimated radiation and static heat loads of 0.18 W and 0.58 W respectively. The occurrence of a stable point of operation in the analysis is given by the intersection between the curve of the total heat load and that of the cryocooler cooling power as a function of temperature of the cryocooler's 4 K stage. The Cu-layer thickness resulting from this finite-element thermal analysis was 4 mm, and a minimum of 5 mm Cu-plating was requested to have some margin.

The Q-switch which limits the maximum achievable surface field in this cavity is attributed to defective regions in poor thermal contact with the surrounding superconductor. At the onset of the Q-switch, these regions may become normal conducting and dissipate more and more of the cavity's stored energy as more power is transmitted into the cavity. One possibility, is the presence of a large number of μm -size defects

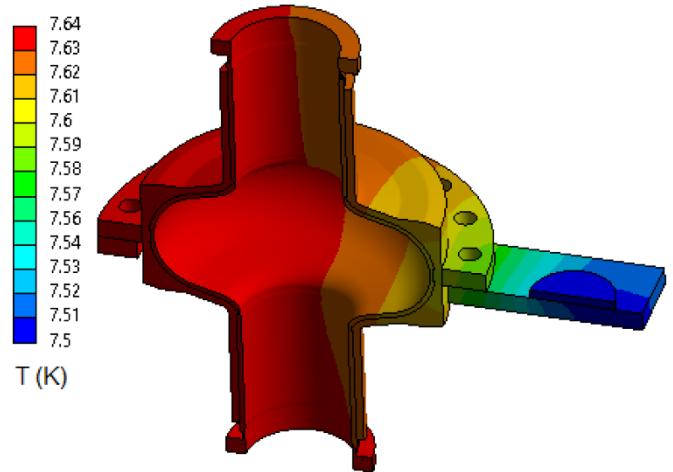


Figure 5. Temperature distribution on the cavity surface and Cu plate with 5 W rf heat load and 0.58 W static heat load, calculated with ANSYS.

distributed uniformly over the cavity surface, given the uniformity of the temperature distribution on the cavity outer surface even with a dissipated power of 5 W. Such a case was evaluated with a steady-state thermal analysis with ANSYS and the temperature distribution is shown in figure 5. A uniform surface resistance value of 460 n Ω was considered for the analysis, corresponding to a total power dissipation of 5 W at $B_p = 22$ mT as it was measured in the experiment. The same values of static and radiative heat leaks and contact thermal conductance used for the analysis determining the minimum Cu thickness were applied. The temperature at the cryocooler location was set to 7.5 K, based on the heat capacity map. Figure 5 indeed shows that the temperature is quite uniform over the whole cavity surface and close to that of the cryocooler, because of the high-conductivity Cu layer. A case in which the additional anomalous rf power loss was concentrated in a single defect was also considered, however it did not result in a stable solution.

The change in the $Q_0(B_p)$ curve above ~ 20 mT indicates an onset of ohmic-type losses as $P_{\text{loss}} \propto H_p^2$ at higher rf field. If such dependence would have continued, without the occurrence of a Q-switch, a $P_{\text{loss}} = 5$ W would have been reached at $B_p = 41$ mT. Such a value of B_p would have met the equivalent accelerating gradient requirement for a single-cell cavity designed for a 1 MeV electron linear accelerator for environmental remediation [11]. However, it should be considered that multiple cryocoolers would still be needed to compensate for additional heat losses due to fundamental power couplers, high-order-mode loads and warm-to-cold transitions in a realistic cryomodule. The origin, size and location of the defective regions are unclear at this stage. One possibility is the contamination of the Nb₃Sn film by the plating solution. Another possibility is related to strain of the Nb₃Sn film given by the differential thermal expansion coefficient between the Cu layer and the Nb layer, since it is well known that the superconducting properties of Nb₃Sn are very sensitive to strain [26]. A finite element mechanical analysis with ANSYS showed that stresses as high as ~ 275 MPa at the irises and ~ 185 MPa

elsewhere on the cell might be applied to the Nb₃Sn-coated Nb, due to the larger thermal contraction of Cu. Given that the yield strength of both oxygen-free Cu and high-purity Nb is ~60 MPa at 300 K, increasing to ~120 MPa and ~600 MPa at 4 K for Cu and Nb respectively [27, 28], plastic deformation might occur in some regions of the cavity. Future work would be needed towards stress management to mitigate the effects of thermal mismatch variations and improving the stiffness of the cryocooled assembly.

6. Conclusion

In summary, we were able to operate a multi-metallic SRF cavity with conduction cooling, using a commercial GM cryocooler, in cw mode up to 29 mT peak surface magnetic field and up to 5 W of power dissipation. In spite of the rigid connection between the cryocooler's 4 K stage and the cavity, the amplitude of the microphonics does not represent an issue, as it was well within what is typically achieved and controlled in SRF accelerator cavities [29, 30], particularly considering the low loaded-Q values ($10^4 - 10^5$) typically required for a low-energy, high-power accelerator.

The copper coating techniques that we used to improve the thermal stability of the cavity do not set a limit on the cavity size, although the availability of a method to obtain a high-purity copper coating by cold-spray would result in a faster process.

To the authors' knowledge, the maximum B_p and P_{loss} values we have reported are the highest ever achieved by a conduction cooled SRF cavity and represent a fundamental stepping stone towards the demonstration of compact, low-cost accelerators for applications in industry, medicine or for university-scale research.

After this work was completed, we became aware of a new report from Fermilab in which $B_p \sim 24$ mT and a P_{loss} of 4 W were achieved in a cryocooler conduction cooled 650 MHz single-cell cavity [31].

Acknowledgments

The authors would like to acknowledge B Golesich at CTC, A Tuck at AJ Tuck Co and D Combs of JLab's machine shop for their expert craftsmanship to produce the cavity's thick Cu shell. We would like to thank our colleagues K Harding and J Henry for the design of the cryocooler test stand, E Daly for helpful discussions on the test setup, JLab's Cavity Production Group for helping with cleaning of the parts and the cavity and D Tucker for helping with the assembly of the test stand. We would also like to thank T Powers for helping with the microphonics measurements. We would like to thank I Parajuli of Old Dominion University for helping with the cavity assembly and sensors installation. We would also like to acknowledge Dr G Ereemeev of Fermilab, formerly at JLab, for allowing access to the Nb₃Sn coating furnace and M Dale of Sumitomo Cryogenics of America for lending us the cryocooler used for this study.

This work is authored by Jefferson Science Associates, LLC under U.S. DOE Contract No. DE-AC05-06OR23 177 and it is partly supported by the Presidential Early Career Award of G Ciovati. The work of U Pudasaini was supported by the DOE Early Career Award of G Ereemeev.

ORCID iD

Gianluigi Ciovati  <https://orcid.org/0000-0001-9316-7704>

References

- [1] Padamsee H 2009 *RF Superconductivity: Science, Technology, and Applications* (New York: Wiley) ch 11 pp 333–387
- [2] Belomestnykh S 2013 Superconducting radio-frequency systems for high- β particle accelerators *Reviews of Accelerator Science and Technology* vol 5 ed Chao A W and Chou W (Singapore: World Scientific) pp 147–84
- [3] Kelly M 2013 Superconducting radio-frequency systems for low-beta particle accelerators *Reviews of Accelerator Science and Technology* vol 5 ed Chao A W and Chou W (Singapore: World Scientific) pp 185–203
- [4] Boulware C 2016 4 K superconducting linacs for commercial applications *2016 North American Particle Conf., Chicago, IL*
- [5] Minehara E J *et al* 1993 Preliminary results of the JAERI FEL superconducting accelerator modules and their cryogenic system *Proc. 6th Int. Conf. RF Superconductivity (SRF'93), Newport News, VA, USA paper SRF93134* (JACoW Publishing Geneva Switzerland) pp 886–94
- [6] Kikuzawa N, Nagai R, Sawamura M, Nishimori N, Minehara E and Suzuki Y 1997 Performance of compact refrigerators system for SRF cavities in the JAERI FEL *Proc. 8th Int. Conf. RF Superconductivity (SRF'97), Padova, Italy paper SRF97C40* (JACoW Publishing Geneva Switzerland) pp 769–73
- [7] Green M A 2015 *IOP Conf. Series: Mater. Sci. Eng.* **101** 012001
- [8] Posen S and Hall D L 2017 *Supercond. Sci. Technol.* **30** 033004
- [9] Kephart R *et al* 2015 SRF, compact accelerators for industry & society *Proc. 17th Int. Conf. RF Superconductivity (SRF'15), Whistler, Canada paper FRBA03* (JACoW Publishing Geneva Switzerland) pp 1467–73
- [10] Barletta W and Borland M 2010 Report of the basic energy sciences workshop on compact light sources, Rockville, md Tech. rep. U.S. Department of Energy
- [11] Ciovati G *et al* 2018 *Phys. Rev. Accel. Beams* **21** 091601
- [12] Dhuley R C, Geelhoed M I, Zhao Y, Terechkin I, Alvarez M, Prokofiev O and Thangaraj J C T to be published Demonstration of CW accelerating gradients on a cryogen-free cryocooler conduction-cooled SRF cavity *IOP Conference Series: Materials Science and Engineering* (<https://lss.fnal.gov/archive/2019/conf/fermilab-conf-19-351-di-ldrd-td.pdf>)
- [13] Duhley R personal communication
- [14] Kneisel P, Ciovati G, Dhakal P, Saito K, Singer W, Singer X and Myneni G 2015 *Nucl. Instrum. Methods Phys. Res. A* **774** 133–50
- [15] Sekutowicz J 2003 Cavities for JLAB's 12 GeV Upgrade *Proc. 20th Particle Conf. (PAC'03), Portland, OR, USA paper TPAB085* (JACoW Publishing Geneva Switzerland) pp 1395–7
- [16] Ereemeev G V, Clemens W A, Macha K, Park H and Williams R S 2015 Commissioning results of Nb₃Sn cavity vapor diffusion deposition system at JLab *Proc. 6th Int. Particle*

- Conf. (IPAC'15), Richmond, VA, USA* (JACoW Publishing Geneva Switzerland) pp 3512–14
- [17] Ereemeev G, Clemens W, Macha K, Reece C E, Valente-Feliciano A, Williams S, Pudasaini U and Kelley M Nb₃Sn multicell cavity coating system at JLAB (Preprint 2001.03823)
- [18] Benvenuti C, Bernard P, Bloess D, Cavallari G, Chiaveri E, Haebel E, Hilleret N, Tückmantel J and Weingarten W 1991 Superconducting niobium sputter-coated copper cavity modules for the LEP energy upgrade *Proc. 14th Particle Conf. (PAC'91), San Francisco, CA, USA* (JACoW Publishing Geneva Switzerland) pp 1023–6
- [19] Ciovati G, Cheng G, Daly E, Ereemeev G, Henry J., Pudasaini U, Parajuli I and Rimmer R 2019 A multi-layered SRF cavity for conduction cooling applications *Proc. 19th Int. Conf. RF Superconductivity (SRF'19), Dresden, Germany, Jun.-Jul. 2019 paper TUP050* (JACoW Publishing Geneva, Switzerland) pp 540–4
- [20] Kanareykin A personal communication
- [21] Hall D, Liepe M, Liarte D and Sethna J P 2017 Impact of trapped magnetic flux and thermal gradients on the performance of Nb₃Sn cavities *Proc. 8th Int. Particle Conf. (IPAC'17), Copenhagen, Denmark, May 2017* (JACoW Publishing Geneva Switzerland) pp 1127–9
- [22] Hovater C, Allison T, Bachimanchi R, Lahti G, Musson J, Plawski T E, Seaton C and Seidman D 2010 Status of the CEBAF energy upgrade RF control system *Proc. 25th Linear Conf. (LINAC'10), Tsukuba, Japan, Sep. 2010, paper MOP095* (JACoW Publishing Geneva Switzerland) pp 280–2
- [23] Padamsee H 2009 High-field Q-slope and quench field *RF Superconductivity: Science, Technology, and Applications* (New York: Wiley) ch 5 pp 192–200
- [24] ANSYS 2019 3D engineering and designing software (ansys.com)
- [25] Dillon A, McCusker K, Dyke J V, Isler B and Christiansen M 2017 *IOP Conf. Series: Mater. Sci. Eng.* **278** 012054
- [26] Godeke A, Hellman F, ten Kate H H J and Mentink M G T 2018 *Supercond. Sci. Technol.* **31** 105011
- [27] Walsh R P, Han K, Toplosky V J and Mitchell R R 2002 *AIP Conf. Proc.* **614** 186–96
- [28] Simon N J, Drexler E S and Reed R P 1992 Properties of copper and copper alloys at cryogenic temperatures Tech rep. NIST Monograph 177
- [29] Powers T, Brock N and Davis G 2019 Microphonics testing of LCLS II cryomodule at Jefferson lab *Proc. SRF'19 (Int. Conf. on RF Superconductivity no 19)* (JACoW Publishing, Geneva, Switzerland) pp 493–498 (<http://jacow.org/srf2019/papers/tup034.pdf>)
- [30] Liepe M and Belomestnykh S 2003 Microphonic detuning in the 500 MHz superconducting CESR cavities *Proc. 20th Particle Conf. (PAC'03), Portland, OR, USA, May 2003 paper TPAB055* (JACoW Publishing Geneva Switzerland) 1326–8
- [31] Dhuley R C, Posen S, Geelhoed M I, Prokofiev O and Thangaraj J C T Demonstration of a cryocooler conduction-cooled superconducting radiofrequency cavity operating at practical cw accelerating gradients arXiv:2001.0782